Chemistry Africa (2024) 7:1921–1933
https://doi.org/10.1007/s42250-024-00894-6

ORIGINAL ARTICLE

Increasing the Functionality of Surgical Masks with Water-Soluble Antibacterial Polymers and MTT Test Studies

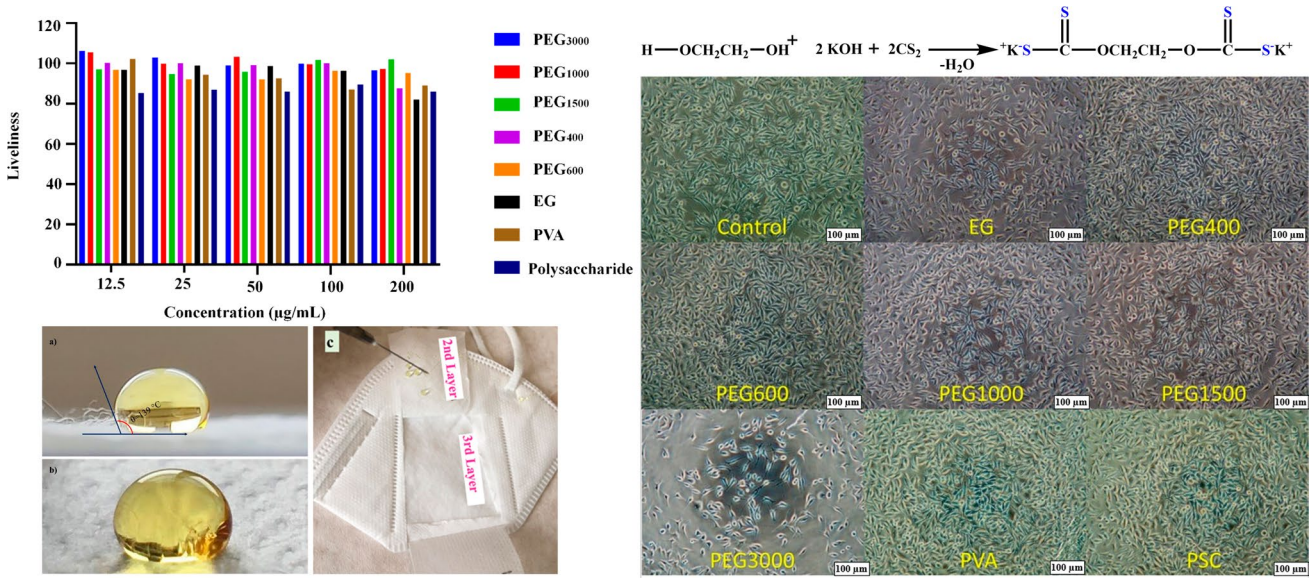
Aysenur Cakmak Oktay[1] · Sevilay Demirci[2] · Aslihan Aycan Tanriverdi[3] · Ali Kurucay[4] · Ahmet Cagri Ata[5]

Received: 12 September 2023 / Accepted: 17 January 2024 / Published online: 29 February 2024
© The Tunisian Chemical Society and Springer Nature Switzerland AG 2024

Abstract

Herein, reversible addition-fragmentation chain transfer (RAFT) agent salts containing water-soluble, antibacterial macro xanthate polyethylene glycol (PEG) were synthesized. Macro xanthate RAFT agent salts were featured by proton nuclear magnetic resonance (^{1}H-NMR) spectroscopy and Fourier transform infrared (FT-IR) spectroscopy. PEG_{1500} Macro Xanthate RAFT agent pure water and PEG_{400} Macro Xanthate RAFT pure water solutions were applied to surgical masks by spraying. Moreover, these polymers were used to determine the minimum inhibitory concentration (MIC) on standard bacterial strains of Gram-positive bacteria and Gram-negative bacteria in the modified Broth MicroDilution method. It was determined that the synthesized polymers prevented the growth of bacteria. Mus musculus mouse fibroblast cells (L-929) were used in the cytotoxicity test of the materials performed by the direct method. It was determined by the Cytotoxicity 3-4,5-dimethyl-thiazolyl-2,5-diphenyltetrazolium bromide (MTT) test that these polymers were not harmful to human health. The biocompatibility of Macro xanthate RAFT agent salts was above 80%.

Graphical Abstract



Keywords Surgical mask · Polymer xanthate · PEG · Biocompatibility · MTT · Antibacterial features

Extended author information available on the last page of the article

1 Introduction

The basic principle of occupational health and safety (OHS) is to protect employees from risks in the workplace and to carry out the work in the safest way [1]. Risks should be reduced or reduced at source using appropriate engineering methods. If the risks cannot be eliminated at the source, personal protective equipment (PPE) is given to the employees. [2, 3] All personal protective equipment must be designed and designed safely and maintained cleanly and reliably. It should fit comfortably in a way that encourages the worker to use it. On the other hand, biodegradable functional polymers are encountered in engineering applications and included in the applications of personal protective equipment. [4, 5] They are known for the structural and molecular features of polymers, such as the material's transition temperature, melting temperature, density, Young's modulus, tensile strength, crystallinity, chain length, and degree of polymerization, and even their biodegradability [6]. Masks are an essential part of PPE. Masks represent the physical respiratory barrier against droplets likely to enter the mouth and nose [7]. There are many types of respirators and surgical masks created to provide users with varying levels of protection. All masks aim to protect against air pollutants such as pollen, pathogens, and chemical fumes. The filtration capacity, and therefore the level of protection against pollutants and pathogens, depends on the materials used and the engineering design. The World Health Organization (WHO) has communicated that wearing a mask is significant for caregivers caring for someone who is sick and is suspected of having severe acute respiratory syndrome infection. Surgical masks were used as a precaution for Covid-19 [8]. Therefore, several mask trials have been conducted to assess the vital importance of wearing a surgical mask to minimize the contagion of the virus. These masks, which are claimed to be the most ineffective of the cloth masks, have some limitations. They include poor filtration efficiency, poor breathability, washability, and reusability. To increase the applicability of these masks, their limitations can be further studied and overcome [9].

In the Bacterial Filtration Efficiency (BFE) test, the threat is provided by *Staphylococcus aureus aerosol* as specified in the ASTM F2101 standard, and the filtering performance of the mask material is measured with the aid of bacteria [10]. The highest BFE result of 99.9% can be obtained when using the ASTM F2101 standard. As is known, masks require approximately 95% BFE. The ASTM F2101 method is a repeatable test procedure. This test can strongly control the expected bacterial aerosol particle size. Comparing various filter materials, evaluated over time, a harmonious set of standards was provided and remained the same for a long time [11].

Surgical masks can provide some form of protection against air and droplets entering the respiratory tract. During the donning and removal of the mask, germs are likely to be transmitted to the limbs that will be in contact with the outside of the mask [11]. The disinfection of reusable masks is quite vital. Cloth masks can be disinfected by washing with detergent, but surgical and N95 masks can only be disinfected with UV. Even if disinfected, the reuse masks will easily become contaminated with pathogenic microbes. Therefore, new masks with antimicrobial activity that can neutralize or destroy infectious microbes can decrease the risk of transmission [12]. Due to increased awareness of outbreaks, reviews have focused on adding antimicrobial activity to masks. That is, masks can be coated or treated with antimicrobial materials. In research, all classes of antimicrobial agents, organic compounds, and metal nanoparticles have provided antimicrobial activity in masks [13, 14].

Polymers with well-defined architectures, predetermined molecular weights, and narrow molecular weight distributions can be produced by the reversible addition-fragmentation chain transfer (RAFT) technique. Well-defined block [15] and graft copolymers [16], periodic or gradient copolymers [17], star and network structured functional end group polymers [18–20], and many other materials have been obtained by a controlled radical mechanism. The controlled radical polymerization (CRP) technique [21, 22] has some advantages in the choice of monomer, the functionality and purity of the resulting polymer, and even the price of the final product. Using RAFT methodology, various polymers with controlled molecular weight and low dispersion have been synthesized with potential applications in different fields such as biotechnology and advanced technologies in biomedical and pharmaceutical fields [23, 24]. RAFT methodology has become more practical due to the research work done by scientists working in the field of polymerization for different vinyl monomers [25].

Herein, Reversible Addition-Fragmentation chain Transfer (RAFT) agent salts containing Macro Xanthate Polyethylene glycol (PEG) were obtained from the reaction of PEG with carbon disulfide (CS_2) and Potassium Hydroxide (KOH). Macro xanthate RAFT agent salts were characterized by proton nuclear magnetic resonance (^{1}H-NMR) spectroscopy and Fourier transform infrared (FT-IR) spectroscopy. Cytotoxicity 3-4,5-dimethyl-thiazolyl-2,5-diphenyltetrazolium bromide (MTT) assay was performed on these salts. Besides, pure water solubility tests were performed and the contact angle of PEG_{400} on the mask layer was determined. The effects of the synthesized substances on some determined bacteria were investigated. Mus musculus mouse fibroblast cells (L-929) were used in the cytotoxicity test of the materials performed by the direct method. PEG_{1500} and PEG_{400} macro xanthate RAFT agent salt pure water solutions were sprayed and applied to the inner layer

of the mask with a needle tip between two types of mask layers with an injector.

2 Materials and Methods

2.1 Materials

Ethylene glycol (EG, $HOCH_2CH_2OH$) (Sigma Aldrich), polyvinyl alcohol 6000 (PVA_{6000}) (Acros Organics), polysaccharide (PSC) (Sigma Aldrich), polyethylene glycol 400, 600, 1000, 1500 ve 3000 (PEG_{400}, PEG_{600}, PEG_{1000}, PEG_{1500} ve PEG_{3000}) (Sigma Aldrich), potassium hydroxide (KOH) (85%, Sigma Aldrich), carbon disulfide (CS_2) (99% Merck), benzoyl chloride (C_6H_5COCI)) (99%, Sigma Aldrich), p-toluoyl chloride (C_7H_8COCI) (98%, Sigma Aldrich), 4-chlorobenzoyl chloride ($C_6H_5COCI_2$) (99%, Sigma Aldrich), dimethyl sulfoxide (DMSO) (99.5%, Sigma Aldrich), 2,2′-azobisisobutyronitrile (AIBN) (99%, Sigma Aldrich) was purchased. Styrene (St) (99%) Sigma Aldrich product was used after distillation. Argon gas was used without purification. Diethyl ether (99.5%, Merck), petroleum ether (99%, Sigma Aldrich), sodium carbonate (99.5%, Sigma Aldrich), methanol (CH_3OH) (99%, Emboy), DMEM High Glucose (Capricorn Scientific), Fetal Bovine Serum (Capricon Scientific), Penicillin- Streptomycin (Capricorn Scientific), MTT (BLDpharm) were purchased.

2.2 Characterizations

Alpha-p Bruker model was used for FT-IR spectrophotometer characterization of the synthesized polymers. ^{1}H-NMR Bruker Avance III HD 600.134 MHz model was used in the NMR spectrophotometer structure illuminations of organic compounds.

2.3 Synthesis of Difunctional Macro Xanthate RAFT Agent Salts

In general, the synthesis of RAFT agents is obtained from the reaction of the xanthate salt with alkyl halides. RAFT agents, Macro xanthate RAFT agent salts containing PEG are obtained from the reaction of PEG with carbon disulfide (CS_2) and Potassium Hydroxide (KOH) (Fig. 1b, Table 1).

2.4 Synthesis of EG, PEG_{400}, PEG_{600}, PEG_{1000}, PEG_{1500} ve PEG_{3000}, PVA_{6000}, and PSC Macro Xanthate RAFT Agent Salts

EG, PEG_{400}, PEG_{600}, PEG_{1000}, PEG_{1500} ve PEG_{3000}, PVA_{6000}, and PSC and potassium hydroxide (KOH) were taken into a 250 mL glass flask separately, mixed in 20 mL benzene (DMSO for just PVA_{6000}) and left to heat. After the system heated under reflux was allowed to cool to room temperature, carbon disulfide (CS_2) was added slowly. After

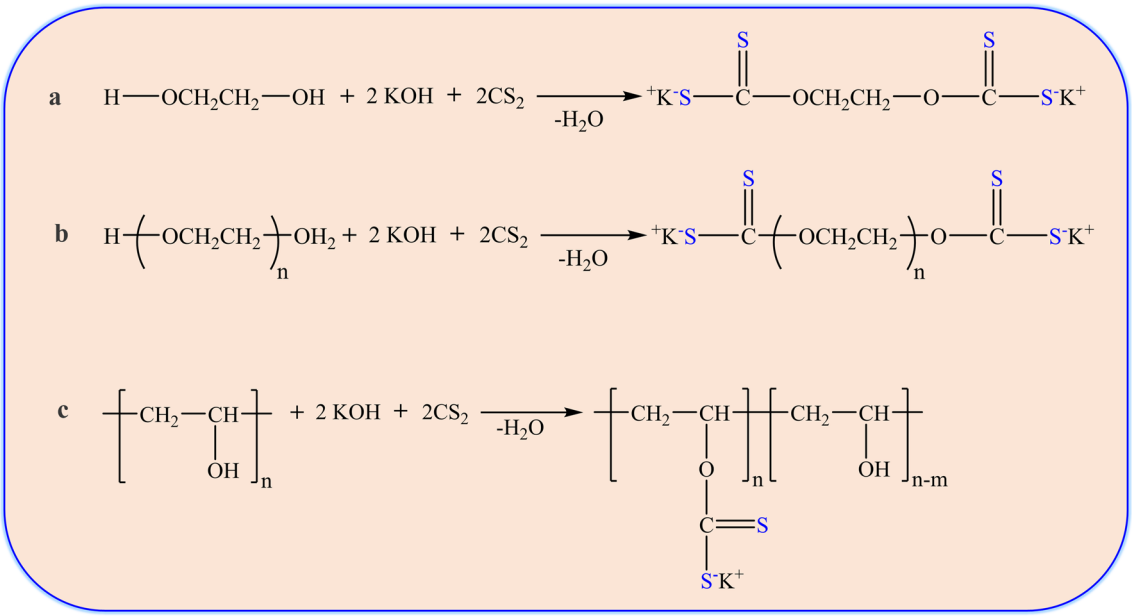


Fig. 1 **a** macro xanthate RAFT agent salt synthesis scheme containing EG, **b** general synthesis scheme of macro xanthate RAFT agent salt containing PEG, **c** macro xanthate RAFT agent salt synthesis scheme containing PVA

Table 1 Materials used in macroRAFT agent xanthate salt synthesis

Materials used during the reaction			Solvent
	KOH	CS_2	
EG 3.1 g (0.05 mol)	5.6 g (0.1 mol)	6 mL (0.1 mol)	Benzene
PEG_{400} 10 g (0.025 mol)	2.8 g (0.05 mol)	12 mL (0.2 mol)	Benzene
PEG_{600} 15 g (0.025 mol)	2.8 g (0.05 mol)	12 mL (0.2 mol)	Benzene
PEG_{1000} 10 g (0.01 mol)	1.12 g (0.02 mol)	2.4 mL (0.02 mol)	Benzene
PEG_{1500} 15 g (0.01 mol)	1.12 g (0.02 mol)	2.4 mL (0.02 mol)	Benzene
PEG_{3000} 15 g (0.005 mol)	1.12 g (0.02 mol)	2.4 mL (0.02 mol)	Benzene
PVA_{6000} 5 g (8.33×10^{-4} mol)	3.73 g (0.066 mol)	4 mL (0.066 mol)	DMSO
PSC 10 g (5×10^{-3} mol)	2.24 g (0.04 mol)	2.5 mL (0.04 mol)	Benzene

For precipitation, a solvent (1:1) mL-mL petroleum ether-diethyl ether was used

PEG Polyethylene glycol; *PVA* Polyvinyl alcohol

the system was stirred for about 20 h, the Macro Xanthate RAFT agent salts containing EG, PEG_{400}, PEG_{600}, PEG_{1000}, $PEG_{1500,}$ and PEG_{3000}, PVA_{6000}, and PSC were formed respectively. The resulting Macro Xanthate RAFT agent salt was filtered through filter paper and allowed to precipitate in another beaker prepared by volume (1:1) mL-mL petroleum ether-diethyl ether. After this mixture was kept in the refrigerator for about 1 day, the prepared (1:1) mL-mL petroleum ether-diethyl ether portion prepared by volume was decanted. EG, PEG_{400}, PEG_{600}, PEG_{1000}, PEG_{1500} ve PEG_{3000}, PVA_{6000}, and PSC macro xanthate RAFT agent salts were dried in a vacuum oven at a temperature of 45–50 °C and a pressure of 200 mbar until constant weight (Fig. 1a, b, and c). Yields 80.4%, 50%, 52.36%, 62.57%, 68.22%, 74.62%, 59%, and 81% respectively. If the values offered by the MestreNova application are given:

For EG, ^{1}H-NMR (400 MHz, D_2O) δ: 3.92 (s, 0H), 3.69 (s, 2H), 3.66–3.55 (m, 12H), 3.54–3.47 (m, 1H).

For PEG_{400}, ^{1}H-NMR (400 MHz, D_2O) δ: 4.72 (dd, J = 3.1, 1.7 Hz, 27H), 4.65 (s, 1H), 3.74–3.65 (m, 4H), 3.69–3.54 (m, 8H), 3.58–3.46 (m, 19H), 3.53 (s, 90H), 3.50–3.45 (m, 1H), 3.42–3.34 (m, 1H), 3.38 (s, 3H), 3.32–3.22 (m, 5H), 3.02 (s, 0H), 2.79–2.66 (m, 3H), 2.66–2.61 (m, 1H), 2.64–2.55 (m, 3H), 2.59 (s, 12H), 1.81–1.76 (m, 0H), 1.78 (s, 4H), 1.22 (d, J = 5.4 Hz, 0H).

For PEG_{600}, ^{1}H NMR (400 MHz, DMSO-*d*6) δ: 4.61 (s, 2H), 4.34–4.27 (m, 1H), 3.79 (s, 4H), 3.64–3.57 (m, 1H), 3.53 (s, 4H), 3.47 (d, J = 5.0 Hz, 1H), 3.45–3.31 (m, 5H), 3.35 (s, 6H). For PEG_{1000}, ^{1}H NMR (400 MHz, DMSO-*d*6) δ: 7.37 (s, 1H), 4.31 (d, J = 5.2 Hz, 1H), 3.64–3.59 (m, 2H), 3.57 (s, 2H), 3.47 (s, 3H), 3.35 (s, 1H), 3.34 (s, 1H).

For PEG_{1500}, ^{1}H NMR (400 MHz, DMSO-*d*6) δ: 4.31 (t, J = 5.0 Hz, 1H), 3.55 (d, J = 15.9 Hz, 11H), 3.47 (d, J = 2.8 Hz, 2H), 3.41 (s, 0H), 3.36 (s, 6H).

For PEG_{3000}, ^{1}H NMR (400 MHz, DMSO-*d*6) δ: 3.84 (s, 7H), 2.74 (s, 2H), 2.63–2.57 (m, 3H), 2.54–2.47 (m, 2H), 1.74 (s, 2H), 1.43 (s, 5H), 1.34 (d, J = 17.0 Hz, 2H).

For PVA_{6000}, ^{1}H NMR (400 MHz, $CDCl_3$-*d*) δ: 7.33–7.18 (m, 7H), 7.26 (s, 6H), 7.10 (d, J = 8.3 Hz, 5H), 6.51 (s, 2H), 4.01 (d, J = 13.1 Hz, 2H), 3.89 (s, 2H), 3.76 (d, J = 1.0 Hz, 5H), 3.55 (t, J = 11.2 Hz, 1H), 3.14 (d, J = 13.9 Hz, 1H), 2.88 (s, 1H), 2.25 (d, J = 17.6 Hz, 2H), 2.17 (d, J = 1.1 Hz, 1H), 1.25 (s, 17H), 0.87 (d, J = 7.0 Hz, 1H), 0.07 (s, 6H), 0.07 (s, 1H), 0.11–0.03 (m, 1H).

2.5 Cytotoxicity 3-4,5-Dimethyl-Thiazolyl-2,5-Diphenyltetrazolium Bromide (MTT) Experiment

High Dulbecco's Modified Eagle's Medium (DMEM) medium with glucose, which contains 10% FBS and 1% Pen-Strep, was used. In the flask, L929 (Mouse Fibroblast) cells were grown at 37 °C and 5% CO_2 atmosphere in an incubator. It was seeded into one plate with 96 wells as to be 10.000 L929 cells in each well. For adhesion and spreading of the L929 cells in the wells, the plate waited in the CO_2 incubator until the next day. Before the addition of each material, a solution was prepared with DMSO at 1 mg ml^{-1} concentration. Then, different concentrations of the solution were prepared by diluting at rations of 12.5, 25, 50, 100, and 200 µg ml^{-1} with the medium.

The waiting medium in the well plate was removed and replaced with 100 µL of the medium containing different compounds. After that, it was incubated for 24 h at 37 °C in a 5% CO_2 incubator until the next day. 5 mg ml^{-1} of MTT dye was dissolved in PBS (Phosphate Buffer, pH: 7.4). After 24 h, the waiting medium was removed from all wells of plates. Hundred µL of the mixture containing 90% DMEM and 10% MTT (5 mg ml^{-1}) was added into each well and incubated for 4 h at the same conditions in the incubator. After incubation, the medium with MTT in the wells was discarded. 100 µL of DMSO was added to each well of the well plates. The plate was read via a spectrophotometer at 540 nm wavelengths immediately after DMSO was added [26].

3 Results and Discussion

3.1 ^{1}H-NMR Spectra of Macro Xanthate RAFT Agent Salts

^{1}H-NMR (Proton nuclear magnetic resonance) spectrum analysis is used to illuminate the structure of compounds and to measure the number of protons they have [27–30]. For EG Macro Xanthate RAFT Agent Salt: Protons of methylene at four signals of 3.51–3.92 ppm have been seen. Since the polymer is multiple units, various $–CH_2$ signals appeared. For PEG_{400} Macro Xanthate RAFT Agent Salt: It can be seen that the protons in $-CH_2$ of the units have a wide band in the range of 3.70–3.27 ppm. For PEG_{600} Macro Xanthate RAFT Agent Salt: The formation of protons of methylene in various signals can be clearly expressed. Low-intensity shifts are observed, singlet at 4.61 ppm and multiplet at 4.31 ppm. Again, broadband is reflected, including singlet and multiplet, in the range of 3.79–3.53 ppm. In addition, it was observed that there were intense singlet, doublet, and multiple signals in the range of 3.47–3.35 ppm. For PEG_{1000} Macro Xanthate RAFT Agent Salt: The $–CH_2$ protons of the PEG unit show a sharp singlet signal at 7.37 ppm, and a low-intensity doublet signal at 4.31 ppm. In addition, while a multiplet broad signal is reflected at 3.62 ppm, intense intensity methylene protons are observed between 3.57 and 3.34 ppm. For PEG_{1500} Macro Xanthate RAFT Agent Salt: A triplet low intensity $–CH_2$ proton shift is observed at 4.31 ppm. Again, a doublet $–CH_2$ protons are reflected at 3.55 ppm and 3.47 ppm. In addition, intense singlet signals between 3.41 and 3.36 ppm are seen. For PEG_{3000} Macro Xanthate for RAFT Agent Salt: The most prominent signals are the singlet shift at the 2.74 ppm signal is two separate multiplet signals at 2.50 ppm. In addition, the low-intensity signals of 1.74 ppm singlet and 1.34–1.43 ppm overlapped singlet and doublet represent the $–CH_2$ protons of PEG units. Finally, It was seen that in the ^{1}H-NMR spectrum of PVA_{6000} Macro Xanthate RAFT Agent salt: –OH exhibited a doublet distinct signal at 4.01 ppm. Doublet signals have low intensity in the range of 2.17–2.25 ppm, belonging to the -CH proton attached to the vinyl alcohol unit. The –CH proton bound to the other unit presented a singlet signal at 1.25 ppm. For $–CH_2$ protons attached to the vinyl alcohol unit, doublet signals at 0.87 ppm and singlet signals at 0.07 ppm were reflected. $–CH_2$ protons bound to the other unit present a singlet signal at 0.07 ppm, while the multiplet signal is at low intensity at 0.06 ppm (Figs. S1–S7).

3.2 FT-IR Analysis of Macro Xanthate RAFT Agent Salts

Similar absorption in the FT-IR spectra of EG, PEG_{400}, PEG_{600}, PEG_{1000}, PEG_{1500}, $PEG_{3000,}$ and PVA_{6000} Macro Xanthate RAFT Agent Salts with the typical FT-IR spectra of PEG and PVA-containing Macro Xanthate RAFT Agent Salts previously reported in the literature [31–33] bands were observed. A strong C–O stretch band appeared at 1646 cm^{-1} at the Fig. S8 ester bond of EG Macro Xanthate RAFT Agent Salt. The bands showing characteristic S=C stretching vibrations are 1568 cm^{-1}, 1350 cm^{-1}, 1350 cm^{-1}, 1348 cm^{-1}, 1342 cm^{-1}, 1340 cm^{-1}, 1340 cm^{-1}. The bands illuminating C-S vibrations are 1354 cm^{-1}, 1247 cm^{-1}, 1247 cm^{-1}, 1246 cm^{-1}, 1241 cm^{-1}, 1239 cm^{-1}, 1317 cm^{-1}, respectively. At the same time, the absorption bands due to the characteristic C–O–C stretching vibrations of the $–OCH_2CH_2–$ unit are 1044 cm^{-1} and 1085 cm^{-1}, respectively. Figs. S8–S14 presents the FT-IR spectra of the PEG_{400}, PEG_{600}, PEG_{1000}, PEG_{1500}, and PEG_{3000} Macro Xanthate RAFT Agent Salts. Strong C-O stretch absorption bands appeared at 1616 cm^{-1}, 1643 cm^{-1}, 1644 cm^{-1}, 1645 cm^{-1}, and 1464 cm^{-1}, respectively, to the formed ester bond. Absorption bands showing characteristic C–O–C stretching vibrations of repeated $–OCH_2CH_2–$ units 948 cm^{-1}, 946 cm^{-1}, 949 cm^{-1}, 951 cm^{-1} and 952 cm^{-1}, 1070 cm^{-1}, 1068 cm^{-1}, 1092 cm^{-1}, respectively is 1142 cm^{-1} and 1099 cm^{-1}. Significant bands confirmed that syntheses had taken place. Finally, Fig. S12 presents the FT-IR spectra of PVA_{6000} Macro Xanthate RAFT Agent Salt. It can be seen that the O–H structure is illuminated with a broad band of 3365 cm^{-1}. A strong C–O stretch absorption band appeared at 1652 cm^{-1} to the formed ester bond. The absorption bands showing repeated $–OCH_2CH_2–$ units and characteristic C–O–C stretching vibrations are 950 cm^{-1} and 1015 cm^{-1}, respectively.

3.3 Test of Solubility in Water

When determining the solubility in water experimentally, the method determines the solubility by balancing between a certain amount of test chemicals and their dissolved form in pure water. Among the significant factors to ensure high-quality resolution determinations are high purity of the test chemical, high purity of water, stability of the test chemical during equilibrium, experiment temperature control, enough shaking, and enough time for the water to reach saturation and full separation to take place [34]. In this study, the solubility of Macro Xanthate RAFT Agent Salts in pure water was tested by mixing technique at room temperature. 0.02 g of EG, PEG_{400}, PEG_{600}, PEG_{1000}, PEG_{1500}, $PEG_{3000,}$ and PVA_{6000} macroxanthate RAFT agent salts were added to 5 ml of distilled water in 8 separate test tubes. It was stirred at 24 °C for 10 min and the colors formed during dissolution

were observed (Table 2). Except for the PVA_{6000} macroxanthate RAFT agent salt, all macroxanthate RAFT agent salts were dissolved in pure water.

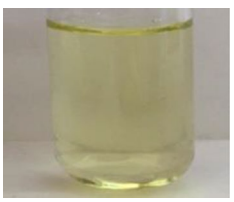
3.4 Contact Angle

Static contact angle [35] can be measured because it is determined to adhere to the surface during applied spraying and exhibits hydrophobic features against the second layer of the mask. PEG_{400} Macro Xanthate RAFT Agent Salt-Pure Water solution and the second layer surface of the mask were used as an example here (Fig. 2). For the measurement of the contact angle (θ), the sample was dropped onto the surface with a syringe. The contact angle presented here is the contact angle measured after 139° ($\theta > 90°$, cohesion > adhesion) liquid-surface contact. The contact angle was measured at 25° C and the average value was reported.

3.5 Effects of Macro Xanthate RAFT Agent Salts on Bacteria

A known opaque polymer containing cationic and hydrophobic groups and its components have a specific task. In the presence of cationic groups, polymers become easier to adhere to the anionic cell membrane of bacteria. Thus, the transport of molecules across the cell membrane takes place. This will disrupt the integrity of the bacterial cell membrane. Moreover, the interaction between the cell membrane and cationic groups is effective in the amphipathic structure of polymers. That is, this property improves bioactive performance. The presence of significant functions mentioned in cationic groups has prompted scientists to investigate the effects on the overall bioactivity of Antimicrobial peptides (AMPs) of cationic groups. Monomers and sulfonium bases functionalized with amino groups have been extensively investigated as cationic options. Palermo et al. [36] reported that amphiphilic copolymers containing primary amine showed higher activity against Gram-negative bacteria and mycobacteria (Mycobacterium smegmatis) of polymers containing quaternary ammonium groups. Hirayama et al. found that sulfonium compounds were more effective against Gram-positive bacteria (S. aureus) than against Gram-negative strains [37]. Especially for the first time, Hu et al. offered polymers in an AB-variable range to the market. It also offered unique antibacterial features against a wide range of clinically known bacterial strains [38]. Ragogna and Gillies proposed phosphonium groups as potential options for enhancing the function of cationic monomers [39]. Kamaruzzaman et al. presented cationic side chain spacers as a new strategy to modulate the molecular structure and antibacterial activity of random AMPs [40]. In the polymer samples, the four-carbon sequestrant in

Table 2 Solubility of macro xanthate RAFT agent salts in pure water

EG macro xanthate RAFT agent salt-pure water	PEG_{400} macro xanthate RAFT agent salt-pure water	PEG_{600} macro xanthate RAFT agent salt-pure water	PEG_{1000} macro xanthate RAFT agent salt-pure water
+ 	+ 	+ 	+ 
PEG_{1500} macro xanthate RAFT agent salt-pure water	PEG_{3000} macro xanthate RAFT agent salt-pure water	PVA_{6000} macro xanthate RAFT agent salt-pure water	Polysaccharide macro xanthate RAFT agent salt -pure water
+ 	+ 	− 	+ 

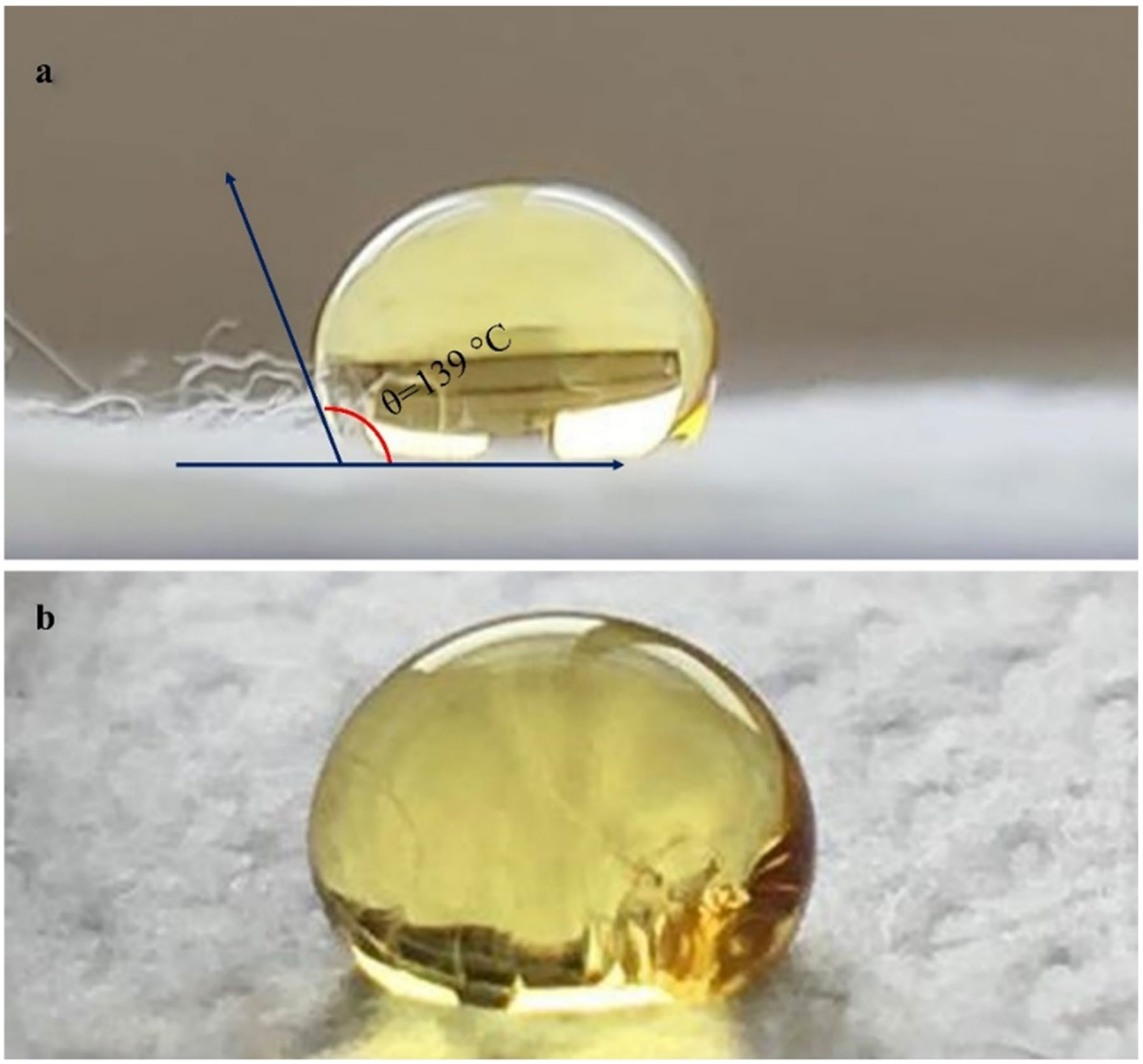


Fig. 2 **a** Contact angle formed by PEG_{400} Macro Xanthate RAFT Agent Salt-Pure Water solution on the 2nd layer of the mask, **b** Close and clear view of the contact formed

4-amino-butyl methacrylate gave the highest antimicrobial activity at minimal hemolytic activity efficiency [41]. Since the other active hydrophobic monomer directly enters the cell and causes membrane disruption, polymers have been prepared with various types of hydrophobic monomers. The polymers were screened to elucidate their effect on the overall selectivity of AMPs [42]. Pu et al. investigated the antibacterial effect of inorganic core sulfobetaine/quaternary ammonium-modified star-shaped poly[2-(dimethylamino) ethyl methacrylate]-based copolymers [43]. Recently, an effective study was carried out on the hemolytic activity of hydrophobic groups of ternary antimicrobial polymers and their effect on antimicrobials. The monomer ratio, degree of polymerization (DPn), hydrophobic monomer carbon length, and chain type of hydrophobic monomer were evaluated on hemolytic activity and antibacterial [44]. Following this study, the most suitable polymers were selected for further cytotoxicity testing. They have high hemocompatibility, but these polymers are toxic to mouse embryonic fibroblasts. This inspired the topic of improving the selectivity of antimicrobial polymers by replacing the hydrophilic groups. Besides the antimicrobial activity of the polymers, hydrophilic groups can reduce unwanted protein complexation [44].

Herein, the effects of the synthesized substances on some determined bacteria were investigated. The modified Broth

Table 3 Dilution values of macro xanthate RAFT agent salts on bacteria

	Staphylococcus Aureus	*Bacillus subtilis*	*Escherichia coli*	*Pasteurella multocida*	*Pseudomonas aeruginosa*
EG	1/8	–	–	1/16	1/8
PEG_{400}	1/8	–	–	–	1/2
PEG_{600}	1/4	–	–	–	–
PEG_{1000}	1/2	–	–	–	–
PEG_{1500}	1/2	–	–	–	–
PEG_{3000}	–	–	–	–	–
PVA_{6000}	–	–	–	1/2	–
PSC	1/8	–	–	1/2	–

MicroDilution method reported by Ericsson and Sherris [45], and Wiegand et al. [46] was used to determine the minimal inhibitory concentration (MIC) of the synthesized substances. Mueller–Hinton Broth (Becton Dickinson, 211,443) was used to prepare the dilutions and as the medium. For this purpose, 1/2, 1/4, 1/8, and 1/16 dilutions were created on U-bottom sterile microplates with the help of Mueller–Hinton Broth by taking 100 µl of the stock solutions of the substances (Table 3). Standard bacterial strains of Gram-positive bacteria *Bacillus subtilis* (laboratory isolate), *Staphylococcus aureus* (ATCC 6538) and Gram-negative bacteria *Escherichia coli* (ATCC 25922), *Pasteurella multocida* (ATCC 12945) and *Pseudomonas aeruginosa* (ATCC 9027) were used. Then, 20 µl of 1/100 dilution of the bacterial suspension prepared from fresh cultures of bacteria and adjusted to 0.5 McFarland turbidity was added to the wells and incubated at 37 °C for 24 h. The tests were run in duplicate and positive and negative controls were also prepared for each substance.

The MIC values of the tested substances were evaluated by measuring the densities of the wells before and after incubation at a wavelength of 450 nm in a spectrophotometer. Considering the results, it can be said that the synthesized substances inhibited the growth of some tested bacteria at different dilutions. None of the substances showed a selective effect on Gram-positive or Gram-negative bacteria. While the substance mentioned as ethylene glycol caused the inhibition of 3 bacterial species tested in different dilutions, PEG_{3000} Macro Xanthate RAFT Agent Salt was not effective on the growth of any of the tested bacteria.

Table 4 The % viability of cells against materials containing different concentrations

%	EG	PEG_{400}	PEG_{600}	PEG_{1000}	PEG_{1500}	PEG_{3000}	PVA_{6000}	PSC
12,5 µg ml^{-1}	96,79,247	100,239	96,76,864	105,478	97,08322	106,1472	102,2028	85,11,857
25 µg ml^{-1}	98,86,393	100,0526	92,05067	99,8321	94,66,355	102,9437	94,34,101	86,9878
50 µg ml^{-1}	98,69,054	99,16,348	91,97,897	103,2723	95,71,701	98,95,022	92,44,429	85,94,323
100 µg ml^{-1}	96,22,605	100,153	96,32,409	99,46,998	101,6592	99,93,506	87,01528	89,43,428
200 µg ml^{-1}	82,03327	87,66,252	95,23,423	97,11,614	102,0213	96,58,009	89,00821	85,86,076

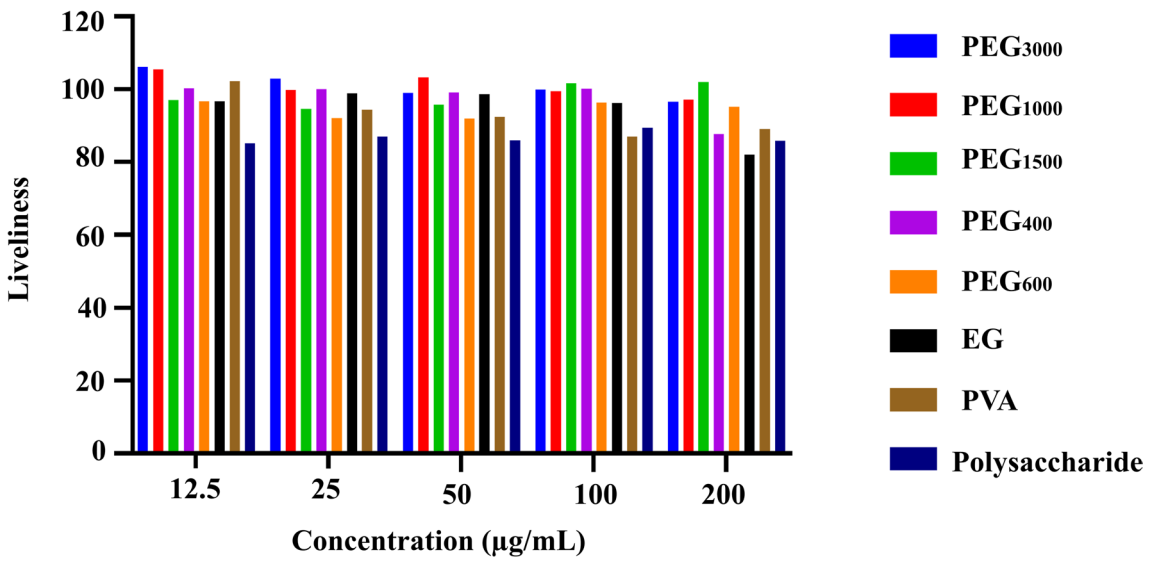


Fig. 3 Graph of cell viability versus materials with different concentrations

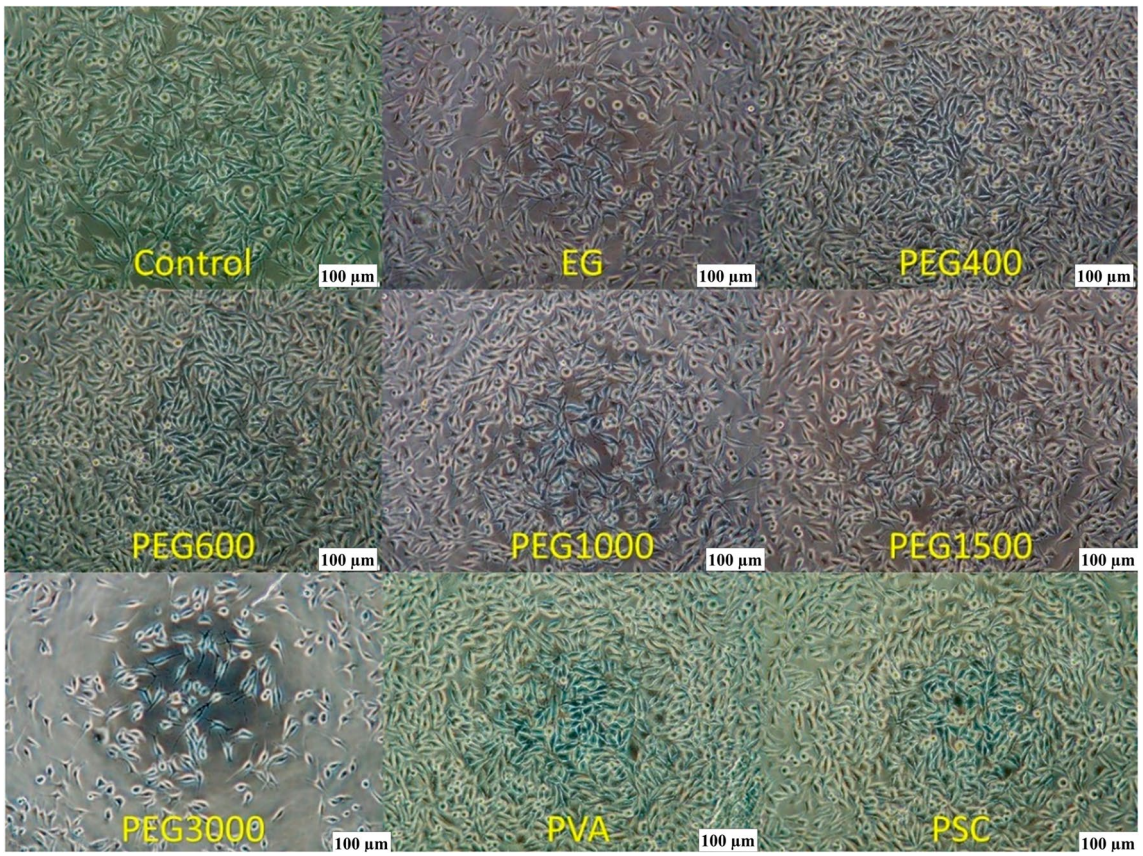


Fig. 4 Images of the effects of the materials on L929 cells at 25 µg/milliliter concentrations after 24 h with an inverted microscope at × 200 times magnification

3.6 Cytotoxicity Test on Mouse Fibroblast (L929) Cells and Cytotoxicity MTT Result

Mus musculus mouse fibroblast cells (L-929) were used in the cytotoxicity test of the materials performed by the direct method [47]. Cell viability result is given in Table 4 and Fig. 3. No toxicity was observed in the concentration range used. The biocompatibility of materials is above 80%. The reduction of cell viability by more than 30% is considered a cytotoxic effect for biomaterials according to ISO-10993-5 (ISO Standard No. 10993-5:2009). The materials were found to be biocompatible.

As can be seen in Fig. 4, the known morphological structures of L929 cells are shown. When the images at 25 µg/milliliter concentrations were compared with the average control image, it was seen that there was no change in the morphology of the cells. (However, the positive control of PEG_{3000} material was compared to PEG_{3000}.) The spherical form in cells can be explained in two ways. These are dead cells or cells that have not yet adhered. However, since the non-adherent cells were removed with the medium in our study, the spherical cells we saw were dead cells. The highest globalization is also seen in PSC.

3.7 Application of PEG_{1500} Macro Xanthate RAFT Agent Salt-Pure Water and PEG_{400} Macro Xanthate RAFT Agent Salt-Pure Water Solutions to Masks

Surgical masks are generally made of degradation-resistant polymeric materials. The masks in question consist of three or four layers of protective polypropylene. It aimed to use surgical masks effectively and safely but also opened the door to pioneering new technologies. Relevant chemical reactions of the main polymers can cause the decomposition of some polymeric parts in surgical masks. Thus, the sequential evolution of C_xH_y fragments (i), by oxidation of visible radical sites (ii), intramolecular H transfer (iii), β fission of carbon–carbon bonds (iv), and water/CO/CO_2 elimination reactions (v), begins as pathways for degradation [48].

In this study, the mask was cut into layers to increase its protection. PEG_{1500} macro xanthate RAFT agent salt-pure water and PEG_{400} macro xanthate RAFT agent salt-pure water solutions were sprayed and applied to the inner layers of the mask with a needle tip between the two types of ready mask layers with an injector. The solution was dropped onto



Fig. 5 **a** The original image of the mask, **b** layers of the mask, **c** spraying on the inside of the 2nd layer of the mask, **d** dispersing the sprayed PEG_{1500} macro xanthate RAFT agent salt-pure water solution sprayed on the inside of the 2nd layer of the mask, **e** dispersing the PEG_{1500} macro xanthate RAFT agent salt-pure water solution sprayed on the outside of the 2nd layer of the mask, **f** the 1st layer of the mask is closed on the 2nd layer

the mask by injecting with the syringe tip. Step-by-step photos are presented (Figs. 5 and 6).

4 Conclusion

Herein, several significant alternative approaches are reviewed to improve the fabrication of surgical masks in membrane technology. In membrane-based technology, it exhibits a high degree of filtration associated with the separation of viruses and micro-aerosol droplets. Appropriate technologies are available for the goal of further increasing the filtration degree of surgical mask basic materials on the market. It is also worth investigating to improve virus adsorption, filtration efficiency, and virus ineffectiveness on the polymeric materials of the surgical mask. Although cost-effectiveness needs to be calculated, approaches may become an option to overcome the shortage of surgical masks. As a result of the tests, the biocompatibility of these polymers was over 80%. As a result, antibacterial features have been gained by spraying surgical masks.

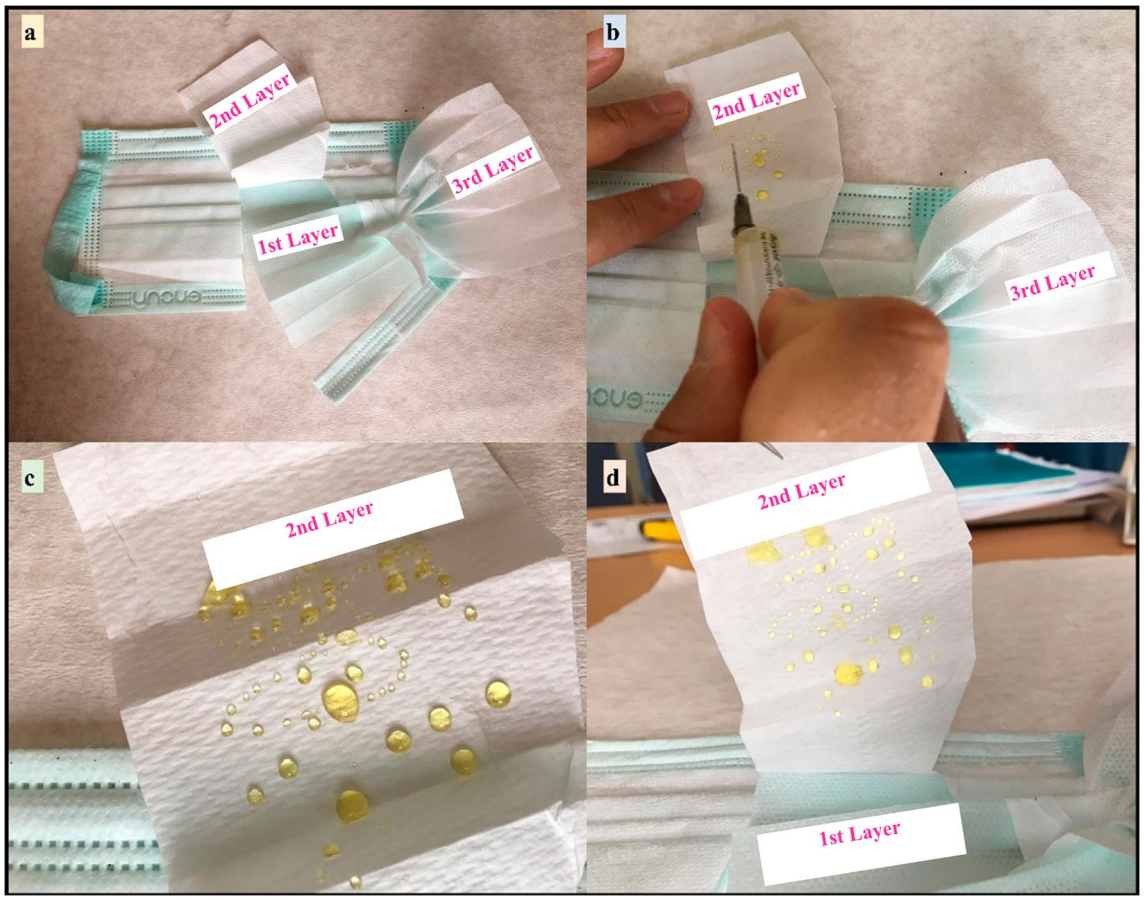


Fig. 6 **a** Layers of the mask, **b** spraying on the inside of the 2nd layer of the mask, **c** Undispersed PEG_{400} macro xanthate RAFT agent salt-pure water solution sprayed on the inside of the 2nd layer of the mask, **d** image of PEG_{400} macro xanthate RAFT agent salt-pure water solution that adheres to the 2nd layer of the mask and does not flow

Supplementary Information The online version contains supplementary material available at https://doi.org/10.1007/s42250-024-00894-6.

Acknowledgements Supporting our team in this study, Instructor we would like to thank Prof. Dr. İsmail Çakmak, Dr. Ümit Yildiko, and Rüstem Ebiri.

Funding The author(s) received no financial support for the research, authorship, and/or publication of this article.

Data availability All data generated or analyzed during this study are included in this published article.

Declarations

Conflict of Interest The author(s) declared no potential conflicts of interest concerning the research, authorship, and/or publication of this article.

References

1. Makin AM, Winder C (2008) A new conceptual framework to improve the application of occupational health and safety management systems. Saf Sci 46(6):935–948
2. Cavazza N, Serpe AJ (2009) Effects of safety climate on safety norm violations: exploring the mediating role of attitudinal ambivalence toward personal protective equipment. J Safety Res 40(4):277–283
3. Casanova LM, Rutala WA, Weber DJ, Sobsey MD (2012) Effect of single-versus double-gloving on virus transfer to health care workers' skin and clothing during removal of personal protective equipment. AJIC 40(4):369–374
4. Van de Velde K, Kiekens P (2002) Biopolymers: an overview of several properties and consequences on their applications. Polym Test 21(4):433–442
5. Karim N, Afroj S, Lloyd K, Oaten LC, Andreeva DV, Carr C, Farmery AD, Kim ID, Novoselov KS (2020) Sustainable personal protective clothing for healthcare applications: a review. ACS Nano 14(10):12313–12340
6. Yang B, Ni H, Huang J, Luo Y (2014) Effects of poly (vinyl butyral) as a macromolecular nucleating agent on the nonisothermal crystallization and mechanical properties of biodegradable poly (butylene succinate). Macromolecules 478(1):284–296
7. Brooks JT, Butler JC (2021) Effectiveness of mask-wearing to control community spread of SARS-CoV-2. Insights 325(10):998–999
8. Wang CJ, Ng CY, Brook RH (2020) Response to COVID-19 in Taiwan: big data analytics, new technology, and proactive testing. Viewpoint 323(14):1341–1342

9. Clase CM, Fu EL, Joseph M, Beale RC, Dolovich MB, Jardine M, Mann JF, Pecoits-Filho R, Winkelmayer WC, Carrero JJ (2020) Cloth masks may prevent transmission of COVID-19: An evidence-based, risk-based approach. Ann Intern Med 173(6):489–491
10. Moyano AJ, Mas CR, Colque CA, Smania AM (2020) Dealing with biofilms of Pseudomonas aeruginosa and *Staphylococcus aureus*: In vitro evaluation of a novel aerosol formulation of silver sulfadiazine. Burns 46(1):128–135
11. Forouzandeh P, O'Dowd K, Pillai SC (2021) Face masks and respirators in the fight against the COVID-19 pandemic: an overview of the standards and testing methods. Saf sci 133:104995
12. Teixeira RF, Balbinot Filho CA, Borges CD (2022) Essential oils as natural antimicrobials for application in edible coatings for minimally processed apple and melon: a review on antimicrobial activity and characteristics of food models food packag shelf. Life 31:100781
13. Rengasamy S, Sbarra D, Horvatin M (2021) Do industrial N95 respirators meet the requirements to be used in healthcare? - A possible solution to respirator shortages during the next pandemic. AJIC 49(9):1194–1196
14. Rengasamy S, Sbarra D, Nwoko J, Shaffer R (2015) Resistance to synthetic blood penetration of national institute for occupational safety and health-approved N95 filtering facepiece respirators and surgical N95 respirators. AJIC 43(11):1190–1196
15. Fang J, Gao X, Luo Y (2020) Synthesis of (hard-soft-hard) x multiblock copolymers via RAFT emulsion polymerization and mechanical enhancement via block architectures. Polymer 201:122602
16. Zakharova NV, Simonova MA, Zelinskii SN, Annenkov VV, Filippov AP (2019) Synthesis, molecular characteristics, and stimulus-sensitivity of graft copolymer of chitosan and poly(N, N-diethylacrylamide). J Mol Liq 292:111355
17. Williams BM, Barone V, Pate BD, Peralta JE (2015) Gradient copolymers of thiophene and pyrrole for photovoltaics. Comput Mater Sci 96:69–71
18. Ishitsuka K, Pagaduan JNM, Kamon Y, Hashidzume A (2020) Mechanical properties of network polymers formed from monodisperse oligo(ethylene glycol)s of different molecular weights through Thiol-Yne reaction. Mater Today Commun 22:100689
19. Tian J, Zhang W (2019) Synthesis, self-assembly and applications of functional polymers based on porphyrins. Prog Polym Sci 95:65–117
20. Uyar Z, Turgut F, Arslan U, Durgun M, Degirmenci M (2019) Synthesis and characterization of well-defined end-chain functional macrophotoinitiators of polystyrene and polyacrylonitrile by RAFT/MADIX polymerization. Eur Polym J 119:102–113
21. Abousalman-Rezvani Z, Eskandari P, Roghani-Mamagani H, Salami-Kalajahi M (2020) Functionalization of carbon nanotubes by combination of controlled radical polymerization and "grafting to" method. Adv Colloid Interface Sci 278:102126
22. Eskandari P, Abousalman-Rezvani Z, Roghani-Mamaqani H, Salami-Kalajahi M, Mardani H (2019) Polymer grafting on graphene layers by controlled radical polymerization. Adv Colloid Interface 273:102021
23. Deepak TL, Mithra GA, Lokesh K, Chandra BS, Subbiah R (2020) Stability of expanded austenite by gas nitriding process on austenitic stainless steel material under low temperature conditions. Mater Today Proc 27:1681–1684
24. Mori H, Endo T (2012) Amino-acid-based block copolymers by RAFT polymerization. Macromol Rapid Commun 33(13):1090–1107
25. Liu Q, Wu H, Zhang L, Zhou Y, Zhang W, Pan X, Zhang Z, Zhu X (2016) RAFT polymerization of N-vinylpyrrolidone mediated by cyanoprop-2-yl-1-dithionaphthalate in the presence of a fluoroalcohol: the possibility of altering monomer properties by hydrogen bonding? Polym Chem 7(11):2015–2021
26. Mosmann T (1983) Rapid colorimetric assay for cellular growth and survival: application to proliferation and cytotoxicity assays. J Immunol Methods 65(1–2):55–63
27. Anderson RJ, McNicholas TP, Kleinhammes A, Wang A, Liu J, Wu Y (2010) NMR methods for characterizing the pore structures and hydrogen storage properties of microporous carbons. J Am Chem Soc 132(25):8618–8626
28. Sripracharat C, Sinthuvanich C, Karpkird T (2022) Cationic cyclodextrin-adamantane poly(vinyl alcohol)-poly(ethylene glycol) assembly for siRNA delivery. J Drug Deliv Sci Technol 68:103052
29. Yildiko U, Ata AC, Cakmak I, Tanriverdi AA (2022) The polyethylene glycol xanthate-mediated synthesis of block copolymers via novel MADIX agents containing azo initiator: effect of PEG chain length on molecular properties. Polym Bull 79:6239–6257
30. Ata AC, Yildiko U, Cakmak I, Tanriverdi AA (2021) Synthesis and characterization of polyvinyl alcohol-g-polystyrene copolymers via MADIX polymerization technique. Iran Polym J 30:885–895
31. Finocchio E, Cristiani C, Dotelli G, Stampino PG, Zampori L (2014) Thermal evolution of PEG-based and BRIJ-based hybrid organo-inorganic materials FT-IR studies. Vib Spectrosc 71:47–56
32. Alibwaini YA, Hemeda OM, El-Shater R, Sharshar T, Ashour AH, Ajlouni AW, Arrasheed EA, Henaish AMA (2021) Synthesis, characterizations, optical and photoluminescence properties of polymer blend PVA/PEG films doped eosin Y (EY) dye. Opt Mater 111:110600
33. Yildiko U, Ata AC, Tanriverdi AA, Çakmak I (2021) Investigation of novel diethanolamine dithiocarbamate agent for RAFT polymerization: DFT computational study of the oligomer molecules. Bull Mater Sci 44:186
34. Birch H, Redman AD, Letinski DJ, Lyon DY, Mayer P (2019) Determining the water solubility of difficult-to-test substances: a tutorial review. Anal chim acta 1086:16–28
35. Sarma M, Abad K, Nguyen D, Ruelas S, Liu K, Thompson J (2021) Investigation of chemical stabilities and contact angle of 3D printed polymers with CO_2 capture solvents to enhance absorber performance. Int J Greenh Gas Control 111:103478
36. Palermo EF, Sovadinova I, Kuroda K (2009) Structural determinants of antimicrobial activity and biocompatibility in membrane-disrupting methacrylamide random copolymers. Biomacromol 10(11):3098–3107
37. Hirayama M (2011) The antimicrobial activity, hydrophobicity and toxicity of sulfonium compounds, and their relationship. Biocontrol sci 16(1):23–31
38. Hu Y, Zhao J, Zhang J, Zhu Z, Rao J (2021) Broad-spectrum bactericidal activity and remarkable selectivity of main-chain sulfonium-containing polymers with alternating sequences. ACS Macro Lett 10(8):990–995
39. Cuthbert T, Harrison T, Ragogna P, Gillies E (2016) Synthesis, properties, and antibacterial activity of polyphosphonium semi-interpenetrating networks. J Mater Chem B 4:4872–4883
40. Kamaruzzaman NF, Tan LP, Hamdan RH, Choong SS, Wong WK, Gibson AJ, Chivu A, Pina MF (2019) Antimicrobial polymers: the potential replacement of existing antibiotics? Int j mol sci 20(11):2747
41. Pham P, Oliver S, Wong EHH, Boyer C (2021) Effect of hydrophilic groups on the bioactivity of antimicrobial polymers. Polym Chem 12:5689–5703
42. Lam MT, FitzGerald PA, Warr GG (2017) Hydrophobic monomer type and hydrophilic monomer ionization modulate the lyotropic phase stability of diblock co-oligomer amphiphiles. Langmuir 338(4):1013–1022

43. Pu Y, Hou Z, Khin MM, Zamudio-Vázquez R, Poon KL, Duan H, Chan-Park MB (2017) Synthesis and antibacterial study of sulfobetaine/quaternary ammonium-modified star-shaped poly[2-(dimethylamino)ethyl methacrylate]-based copolymers with an inorganic core. Biomacromol 18(1):44–55
44. Phuong PT, Oliver S, He J, Wong EHH, Mathers RT, Boyer C (2020) Effect of hydrophobic groups on antimicrobial and hemolytic activity: developing a predictive tool for ternary antimicrobial polymers. Biomacromol 21:5241–5255
45. Ericsson HM, Sherris JC (1971) Antibiotic sensitivity testing. report of an international collaborative study. Acta pathol microbiol Scand B Microbiol Immunol 21:217
46. Wiegand I, Hilpert K, Hancock REW (2008) Agar and broth dilution methods to determine the minimal inhibitory concentration (MIC) of antimicrobial substances. Nat protoc 3:163–175
47. Teixeira RR, Barbosa LC, Maltha CR, Rocha ME, Bezerra DP, Costa-Lotuf LV, Pessoa C, Moraes MO (2007) Synthesis and cytotoxic activity of some 3-benzyl-5-arylidenefuran-2(5H)-ones. Molecules 12(5):1101–1116
48. Selvaranjan K, Navaratnam S, Rajeev P, Ravintherakumaran N (2021) Environmental challenges induced by extensive use of face masks during COVID-19: a review and potential solutions. Environ Chall 3:100039

Springer Nature or its licensor (e.g. a society or other partner) holds exclusive rights to this article under a publishing agreement with the author(s) or other rightsholder(s); author self-archiving of the accepted manuscript version of this article is solely governed by the terms of such publishing agreement and applicable law.

Authors and Affiliations

Aysenur Cakmak Oktay[1] · Sevilay Demirci[2] · Aslihan Aycan Tanriverdi[3] · Ali Kurucay[4] · Ahmet Cagri Ata[5]

✉ Sevilay Demirci
incesevilay@gmail.com

[1] Department of Occupational Health and Safety, Graduate School of Natural and Applied Sciences, Kafkas University, 36100 Kars, Turkey

[2] Department of Chemical Engineering, Faculty of Engineering and Architecture, Kafkas University, 36100 Kars, Turkey

[3] Department of Chemistry, Faculty of Arts and Sciences, Kafkas University, 36100 Kars, Turkey

[4] Department of Chemistry, Faculty of Science, Inonu University, 44280 Malatya, Turkey

[5] Department of Physical Chemistry, Graduate School of Natural and Applied Sciences, Kafkas University, 36100 Kars, Turkey